

Evolution of Iridium-Based Molecular Catalysts during Water Oxidation with Ceric Ammonium Nitrate

Douglas B. Grotjahn,^{*,†} Derek B. Brown,[†] Jessica K. Martin,[†] David C. Marelius,[†] Marie-Caline Abadjian,[†] Hai N. Tran,[†] Gregory Kalyuzhny,[†] Kenneth S. Vecchio,[‡] Zephen G. Specht,[†] Sara A. Cortes-Llamas,^{†,§} Valentin Miranda-Soto,[†] Christoffel van Niekerk,[†] Curtis E. Moore,[‡] and Arnold L. Rheingold[†]

[†]Department of Chemistry and Biochemistry, 5500 Campanile Drive, San Diego State University, San Diego, California 92182, United States

[‡]Department of NanoEngineering and [§]Department of Chemistry and Biochemistry, University of California, San Diego, La Jolla, California 92093, United States

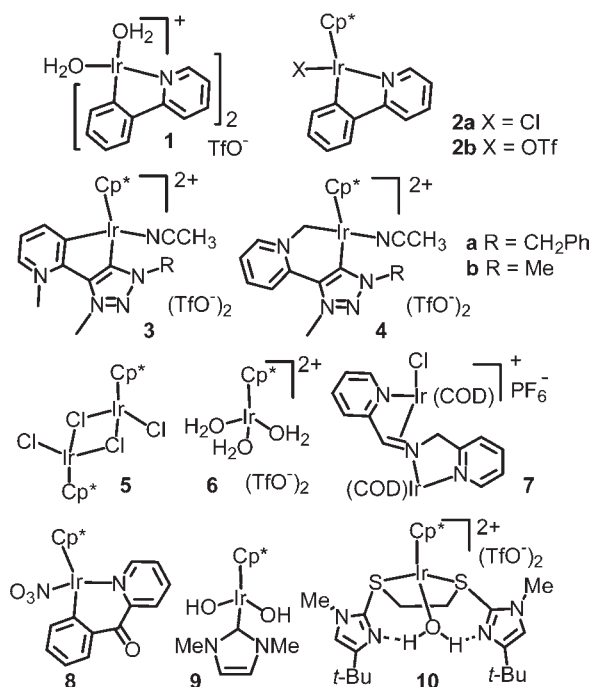
S Supporting Information

ABSTRACT: Organometallic iridium complexes have been reported as water oxidation catalysts (WOCs) in the presence of ceric ammonium nitrate (CAN). One challenge for all WOCs regardless of the metal used is stability. Here we provide evidence for extensive modification of many Ir-based WOCs even after exposure to only 5 or 15 equiv of Ce(IV) (whereas typically 100–10000 equiv are employed during WOC testing). We also show formation of Ir-rich nanoparticles (likely IrO_x) even in the first 20 min of reaction, associated with a Ce matrix. A combination of UV–vis and NMR spectroscopy, scanning transmission electron microscopy, and powder X-ray diffraction is used. Even simple IrCl₃ is an excellent catalyst. Our results point to the pitfalls of studying Ir WOCs using CAN.

One compelling scenario for solving world energy needs hinges on efficient formation of H₂ and O₂ from water using sunlight.^{1a} Breaking down this important and extremely challenging goal into parts, the oxidation of water to produce O₂, electrons, and protons is widely considered the bottleneck to a practical water-splitting scheme and is the focus of intense effort worldwide.¹ Since 1982,^{2a} Ru complexes² have been at the forefront of water oxidation catalysts (WOCs), followed by complexes of Mn.³ More recently, in 2008,^{4a} the first discrete Ir-based WOC, **1** (Chart 1), was followed by Cp*Ir-based systems **2a,b**^{4b} as well as simpler complexes such as **5** and **6**,^{4c,d} carbonyl analogue **8**,^{4d} chelating carbene complexes **3a** and **4a**,^{4e} unidentate carbene complex **9**,^{4f} chelating carbene or alkoxide complexes related to both **2a** and **9** (not shown),^{4g,h} and binuclear (COD)Ir system **7**.⁴ⁱ These new systems, along with other new Fe- or Co-based catalysts,⁵ represent breakthroughs in the WOC field, because they show that metals other than Ru or Mn can catalyze water oxidation. Our ongoing interest in Cp*Ir chemistry⁶ led us to examine Ir-based WOCs, including **10**.^{6c} Because Ir is a precious metal, its large-scale application would require very robust and active catalysts.⁷

Here we report findings pointing to rapid modification of Ir WOCs by Ce(IV), leading to ligand oxidation products and Ir-rich nanoparticles (NPs), likely IrO_x or IrO₂, which are themselves well-known and highly efficient WOCs of continued interest.⁸ The question of stability of Ir-based WOCs has been considered,^{4b,c,f,hi} but direct evidence of WOC modification and/or NP formation has been lacking, and in fact in the more thorough studies (e.g., ref 4c) some negative evidence has been given. Our data do not address whether

Chart 1. Organometallic Iridium Water Oxidation Catalysts



IrO_x NPs are the sole WOC under conditions employed, but they do highlight the need to do more than measure O₂ evolution from aqueous Ce(IV) for evidence of robustness of a molecular catalyst.

As summarized above, creating efficient WOCs is a major scientific and technical obstacle. The long-term goal is to use sunlight for the process, but for initial studies Ce(IV) in the form of ceric ammonium nitrate (CAN) is widely used as a sacrificial one-electron oxidant (e.g., see refs 2k,l in the Supporting Information (SI), 3c, and 4). The ability of Ce(IV) to oxidize organic compounds is well-known,⁹ and its role in WOC reactions is receiving increasing scrutiny.^{4c,10}

Typical CAN-based WOC experiments involve adding catalyst to aqueous CAN solutions, where CAN/catalyst ratios are

Received: April 5, 2011

Published: November 07, 2011

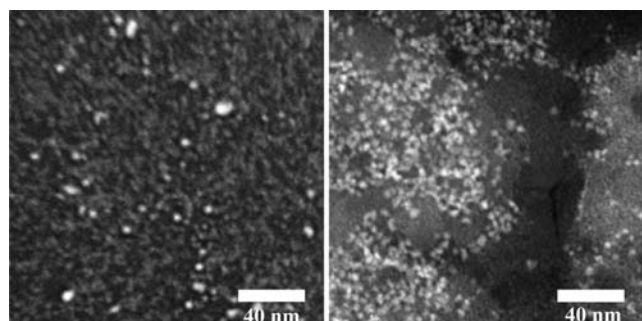


Figure 1. STEM images: (left) authentic IrO_x NPs; (right) sample removed 15 min after **2a** was added to CAN, $[\mathbf{2a}]_0 = 1.35$ mM, $[\text{CAN}]_0 = 78$ mM, $[\text{CAN}]/[\mathbf{2a}] = 58$. Note association of Ir-rich NPs (~ 2 nm bright dots) with Ce-rich matrix. See Figure S16 for UV–vis under these same conditions, and Figures S4–S9 for STEM and EDX data from **1**, **3b**, **6**, IrCl_3 , and IrO_x NPs.

100–10000. We started our investigations under similar conditions, adding solutions¹¹ of WOCs to aqueous CAN at the same initial concentrations used by previous workers (172^{4a} or 78 mM;^{4b} see for example Figure S27¹²). As detailed below, using Clarke electrodes, O_2 production was observed, but we also noted that the orange color of CAN changed as the mixtures became various shades of pale violet, bluish, or olive-green, depending on the catalyst used and reaction progress. Because Ce(III) is colorless,^{13a} we hypothesized that the colors seen were somehow derived from the catalyst.

Indeed, inspection of literature^{8b,c,f,h} revealed colors for IrO_2 or IrO_x NPs described as blue, purple, or blue-gray, and also distinctive UV–vis absorptions between 550 and 700 nm, depending on additive and perhaps size or aggregation.^{8a,c,f}

To gain additional evidence for the presence of IrO_x NPs, we used scanning tunneling electron microscopy (STEM) and powder X-ray diffraction (PXRD).¹² STEM images of succinate-stabilized^{8c} or unstabilized IrO_x NPs^{8f} of ~ 2 –10 nm diameter were successfully obtained (Figure 1, left). Energy-dispersive X-ray (EDX) analysis confirmed the presence of Ir. Samples from water oxidation mixtures ($[\text{WOC}]_0 = 1.35$ mM for IrO_x NPs, **1**, **2a**, **3b**,^{12a} **6**, or **9**; $[\text{WOC}]_0 = 2.0$ mM for IrCl_3) did not show evidence of free Ir-rich NPs, but rather NPs associated with Ce (Figures 1, right, and S4–S9). Our attempts to separate Ir and Ce materials according to reviewer suggestion were neither successful using dialysis nor ultracentrifugation (80 000 rpm), though we did find that Ir-rich NPs survive lyophilization. We hypothesize that the Ir and Ce agglomerate, forming species containing but not strictly identical to IrO_x NPs made without Ce present,^{8b,c,f} nor resembling bulk IrO_2 . As to possible routes of agglomeration, both Ce(III) and -(IV) ions form dimers in solution and the solid state,¹³ where oxide or hydroxide bridging ligands are known. Furthermore, hypothesized Ir–Ce association during electron transfer^{4c,10b} might be a route toward heterometallic agglomeration. Related interactions of the form Ce–OH–Ru were recently suggested.^{10a} Regardless of the precise mechanism, it makes sense that there should be Ce–Ce and Ce–Ir interactions during catalysis.

Furthermore, UV–vis spectra (Figures 2, S14–S16) of water oxidation reaction mixtures using a wide variety of catalysts¹² show the growth of absorbances centered between 550 and 650 nm,^{14a} which agrees with the range of absorption maxima recorded for IrO_2 or IrO_x NPs.^{8b,c,f} Control experiments (Figure S13) verified that before oxidation the catalysts examined did not absorb at 550–700 nm.

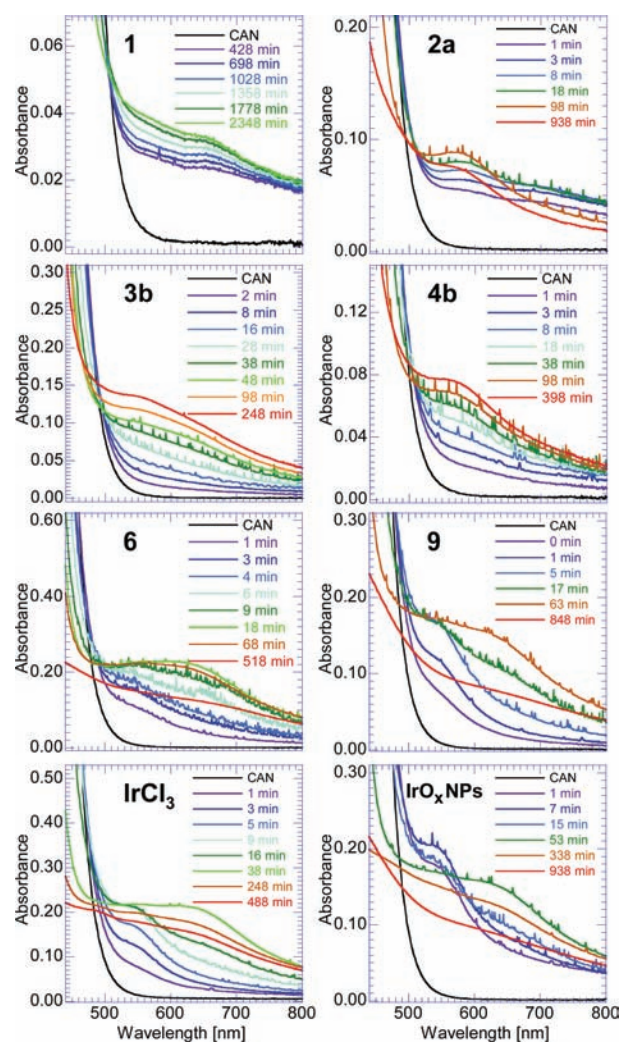


Figure 2. UV–vis absorption spectra obtained at various times after the catalyst indicated was added to freshly prepared aqueous solutions of CAN ($[\text{CAN}]_0 = 75.8$ –78.9 mM).¹² The amount of catalyst added was such that $[\text{catalyst}]_0 \approx 0.05$ mM (range 0.050–0.053 mM), $[\text{CAN}]_0/[\text{catalyst}]_0 = 1560$. The absorbances with maxima between 550 and 650 nm are ascribed to IrO_x NPs (see text). Small spikes on the traces are caused by gas bubbles (O_2 , as detected in separate experiments; to see the similarity of O_2 evolution progress using **3b** and IrO_x NPs, see Figure S27).

Assuming that the molar absorptivity of “pure” IrO_x NPs^{8f} is the same for NPs formed from WOCs and CAN, for reactions in Figure 2 one could expect the absorbance due to IrO_x NPs should be 0.032 AU,^{14b} which is in the range seen for all catalysts except perhaps **1**.

Significantly, even when IrCl_3 is used, we see similar results, though for this catalyst as well as **6** and **9** there appears to be a rise in absorbance near 560 nm, followed by its decline and concomitant rise of a second absorption near 610–620 nm. The changes over time suggest evolution of the NPs mixture, perhaps involving Ce. Notably, even when authentic IrO_x NPs are used at $[\text{IrO}_x]_0 = 0.05$ mM, within 1 h the original 580 nm band is replaced by one closer to 620 nm,^{14a} consistent with changes in NP environment suggested by images (Figure S8) of authentic IrO_x NPs closely associated with Ce-rich material after mixing with CAN.

Another series of experiments was designed to explore the role of initial catalyst concentration. Here, to 78 mM aqueous solutions of

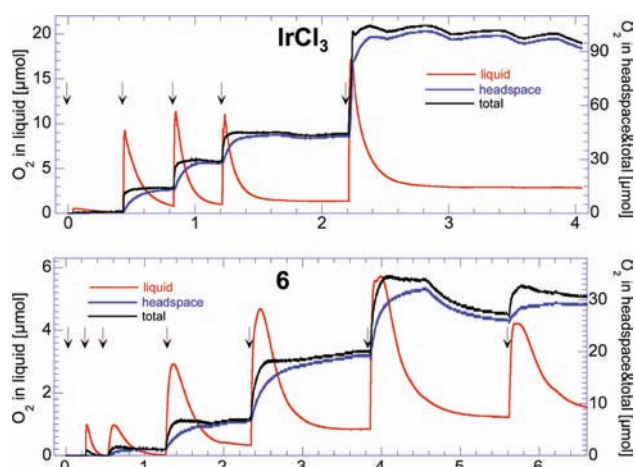


Figure 3. Effects of stepwise reactions of ca. 5 mol of CAN per mole of Ir catalyst. O_2 amounts in liquid and headspace were measured using two Clarke electrodes. Arrows point to times at which more CAN was added. (a, top) To CAN ($78.4 \mu\text{mol}$) in water (7.0 mL) was added IrCl_3 ($15 \mu\text{mol}$) in water (0.5 mL) at time = 0.0 min; $<1 \mu\text{mol}$ of O_2 was seen. In contrast, at $t = 26, 50,$ and 73 min, more CAN ($75.7\text{--}81.0 \mu\text{mol}$) produced close to theoretical amounts of O_2 within 5 min each time. The need to consider diffusion of freshly formed O_2 from liquid to headspace over ca. 15 min is apparent. A final addition at $t = 133$ min of CAN ($237.1 \mu\text{mol}$) is also shown. Conclusion: only about 5 mol of Ce(IV) per mole of Ir is needed to generate active catalyst. (b, bottom) A similar experiment with **6** ($15.6 \mu\text{mol}$) shows very little O_2 ($<10\%$ of theory) after additions at 2 and 15 min, slightly more at 32 min, and ca. 50, 80, and 100% of theoretical O_2 after 76, 141, and 232 min. Conclusion: approximately 15 mol of Ce(IV) is needed per mole of Ir to generate active WOC, suggesting that Cp^* ligand consumes some Ce(IV). Similar experiments with **2a**, **3b**, **4b**, and **9** (Figures S18–S22) showed no or little O_2 until 20–30 equiv of Ce(IV), suggesting that added organic ligand consumes oxidant.

CAN was added **2a** so as to make mixtures with $[\mathbf{2a}]_0 = 1.35, 0.45, 0.15, 0.05,$ and 0.0157 mM. In this series of 3-fold dilutions, even at the lowest concentration of added **2a**, detectable growth of a UV–vis peak centered near 580 nm was seen (Figure S14). The maximal absorbance at 580 nm was approximately proportional to the amount of **2a** added (Figure S14). The Crabtree group reported^{4c} water oxidations using $[\mathbf{2a}]_0 = 0.001\text{--}0.020$ mM, typically 0.005 mM; thus, the 0.0157 mM condition is within the range of concentrations used. At a still lower concentration ($[\mathbf{2a}]_0 = 0.0052$ mM), one cannot say that there is a distinctive feature at 580 nm (Figure S14), but as can be appreciated from Figure S14e, the data for this experiment (lower left point) fit the trend seen over a 30-fold range in $[\mathbf{2a}]_0$. As for the speed at which absorbance at 580 nm is detectable, *within minutes of adding sufficient catalyst* to make $[\mathbf{2a}]_0 = 0.05$ mM (Figure 2), absorbance at 580 nm appeared and became most intense within about 3 h, and then slowly (hours) diminished. Complex **1** is the slowest to develop absorbance between 600 and 650 nm, but it is also the slowest of the reported catalysts. Significantly, literature reports⁴ on the effectiveness of **1–9** show O_2 production over at least 1 h, with a tapering off in O_2 production. Results very similar to those for **2a** were obtained using **6** over a range of initial concentrations from 0.050 to 0.005 mM (Figure S15); this simple catalyst was found by Savini et al. to be 2–3 times faster at forming O_2 than either **2a** or **8**.^{4d}

The evidence of catalyst instability prompted us to gain insight into the *early evolution* of WOCs. Thus, we performed novel experiments in which WOCs were exposed to *limited amounts* of CAN

(5 mol/mol of catalyst), followed stepwise by additional doses of CAN, to see at what point O_2 formed. Oxygen production is typically measured using an electrode,^{2b,4b,c} but pressure-,^{4a} volumetric-,^{4c,i} or fluorescence-based^{4c} assays have also been used. Some workers measure O_2 dissolved in the reaction mixture,^{4b,c} but most examine the headspace.^{2b,4a,4e} We chose to assess O_2 levels using a custom-made cell with a Clarke electrode in each phase (Figure S17). *In this manner we could observe both O_2 formation in the first few seconds as it occurred in the reaction mixture, and over longer periods of time (minutes) as O_2 diffused into the headspace.* Surprisingly, we have not seen a discussion of the consequences of only being to determine O_2 levels in only one phase at a time. Our data (Figure 3) show that, using conventional magnetic stirring, equilibration takes on the order of 15 min.

More significantly, our data indicate that several equivalents of oxidant are needed before O_2 is formed, with the number generally increasing as the number of organic coligands increases. For example, IrCl_3 was added to CAN (5 equiv), and virtually no O_2 was produced, consistent with suggestions^{4c,i} that some oxidant is needed to create the actual WOC. Three subsequent additions of CAN (5 equiv each) *each produced instantaneous bursts of O_2 in the liquid* (Figure 3a). A similar experiment with **6** required several doses of CAN (totaling ~ 15 mol of CAN per mole of Ir) to lead to significant amounts of O_2 after each addition (Figure 3b), whereas experiments with **2a**, **3b**, **4b**, and **9** (Figures S18–S22) suggested that as much as 30 mol of CAN per mole of Ir was needed.^{12,15} In complete contrast, *when authentic acidified IrO_x NPs^{3f} were used* (Figure S24), O_2 was formed from the very first 5 mol of CAN. Organic ligands appear to consume some CAN as part of activating WOCs.

Thanks to an excellent reviewer suggestion, we obtained very direct evidence of the effects of CAN on molecular WOCs. Emulating conditions of Figures 3 and S18–S24, to solutions of **1**, **3b**, **4b**, **6**, and **9** (~ 1.35 mM in D_2O for NMR and MS, H_2O for UV–vis) were added portions of CAN (first 1, then 4, and finally 10 equiv). Changes in ^1H NMR, ESI-MS, and UV–vis spectra following these stepwise additions were profound.^{12b} Most NMR peaks were sharp, not broadened as one might expect for paramagnetic^{4b} Ir(IV) intermediates. In all cases, some changes were apparent even after only 1 equiv of CAN. For example, in the case of **4b** (**3b** was similar), after 1 and 5 total equiv of CAN, only 84% and 31% of original catalyst remained,^{12c} and significant amounts (7 and 19%) were formed of a species tentatively identified^{12b} as having one Cp^* CH_3 group oxidized¹⁶ to a $-\text{CH}_2\text{OH}$; however, by the time 15 equiv of CAN had been added, peaks for these species were replaced by a profusion of uncharacterizable resonances (Figure S28-15-a–h). Two chemically significant peaks were seen at 8.24 and 2.09 ppm, identified as formic and acetic acids.^{12b} The presence of one- and two-carbon fragments after only 15 equiv of CAN in combined amounts ranging from 0.43 to 0.92 mol per mole of original complex^{12c} along with reports of CO_2 ^{4a} from **1** and CAN are evidence of deep-seated ligand oxidation, which our data show occur early in WOC + CAN reactions.^{12d} Furthermore, UV–vis data using **3b** (Figures S25 and S26) show that a rise in absorption between 580 and 630 nm occurs only as 10–25 equiv of CAN are added and stops near a value one would expect if all Ir had been converted to IrO_x NPs, consistent with changes in O_2 evolution, NMR, and MS data.

In summary, novel stepwise addition experiments show that addition of CAN (even <15 equiv) to Ir WOCs **1**, **3b**, **4b**, **6**, and **9** creates new molecular species, including ligand-oxidized complexes as well as formic and acetic acids, identified for the first time. At this stage, little O_2 evolution occurs. With more CAN, a rise in UV–vis absorption identical or very similar to that of IrO_x is seen, and O_2 evolution increases. If the rise in UV absorption is due to molecular

species, because 10–25 equiv of oxidant are needed, the changes wrought by CAN must be more extensive than oxidation of the metal alone to Ir(IV) or Ir(V).^{14a} After 58 equiv of CAN is added, the UV–vis absorption persists, and imaging Ir-rich NPs from reactions of $[\text{WOC}]_0 = 1.35 \text{ mM}$ was done for five Ir-based WOCs. At the higher concentrations needed to see directly NPs or PXRD patterns, in this study we see evidence of Ir–Ce agglomeration or association, which occurs even starting with authentic IrO_x NPs. At lower Ir concentrations, our UV–vis data indicate that, within minutes, some portion of molecular Ir-based WOCs are converted to species with UV–vis absorbances in the same range as those seen for independently synthesized IrO_x NPs. Our data show for the first time profound changes to the molecular WOCs studied with even <15 equiv of CAN. Ir-based catalysts **1**, **2a**, **3b**, **4b**, **6**, and **9** in the presence of Ce(IV) clearly evolve to new species, which hopefully can be avoided by using electrochemical^{4h} or other oxidants, along with improved ligand and catalyst design. Given the importance of water oxidation in solar energy schemes, development of truly robust^{5c} catalyst systems remains a very worthy goal, being pursued in many laboratories.

■ ASSOCIATED CONTENT

S Supporting Information. Details of new compound preparation, CIF of **3b**, procedures, and UV–vis, STEM, PXRD, NMR, and MS data from WOC reactions. This material is available free of charge via the Internet at <http://pubs.acs.org>.

■ AUTHOR INFORMATION

Corresponding Author

grotjahn@chemistry.sdsu.edu

Note

⁵Fulbright Scholar on leave from Universidad de Guadalajara.

■ ACKNOWLEDGMENT

We thank San Diego Cleantech Innovation and Commercialization Program and SDSU for support, NSF for SDSU NMR facilities (MRI CHE-0521698), Aaron G. Nash for related experiments, and Fulbright for their award to S.C.-L.

■ REFERENCES

- (1) (a) Lewis, N. S.; Nocera, D. G. *Proc. Natl. Acad. Sci. U.S.A.* **2006**, *103*, 15729. (b) Sala, X.; Romero, L.; Rodriguez, M.; Escriche, L.; Llobet, A. *Angew. Chem., Int. Ed.* **2009**, *48*, 2842. (c) Brimblecombe, R.; Dismukes, G. C.; Swiegers, G. F.; Spiccia, L. *Dalton Trans.* **2009**, 9374.
- (2) (a) Gersten, S. W.; Samuels, G. J.; Meyer, T. J. *J. Am. Chem. Soc.* **1982**, *104*, 4029. (b) Zong, R.; Thummel, R. P. *J. Am. Chem. Soc.* **2005**, *127*, 12802. (c–m) See SI for 11 more references.
- (3) (a) Brimblecombe, R.; Kolling, D. R. J.; Bond, A. M.; Dismukes, G. C.; Swiegers, G. F.; Spiccia, L. *Inorg. Chem.* **2009**, *48*, 7269. (b) Poulsen, A. K.; Rompel, A.; McKenzie, C. J. *Angew. Chem., Int. Ed.* **2005**, *44*, 6916. (c) Tagore, R.; Chen, H.; Zhang, H.; Crabtree, R. H.; Brudvig, G. W. *Inorg. Chim. Acta* **2007**, *360*, 2983. (d) Ramaraj, R.; Kira, A.; Kaneko, M. *Chem. Lett.* **1987**, 261.
- (4) (a) McDaniel, N. D.; Coughlin, F. J.; Tinker, L. L.; Bernhard, S. *J. Am. Chem. Soc.* **2008**, *130*, 210. (b) Hull, J. F.; Balcells, D.; Blakemore, J. D.; Incarvito, C. D.; Eisenstein, O.; Brudvig, G. W.; Crabtree, R. H. *J. Am. Chem. Soc.* **2009**, *131*, 8730. (c) Blakemore, J. D.; Schley, N. D.; Balcells, D.; Hull, J. F.; Olack, G. W.; Incarvito, C. D.; Eisenstein, O.; Brudvig, G. W.; Crabtree, R. H. *J. Am. Chem. Soc.* **2010**, *132*, 16017. (d) Savini, A.; Bellachioma, G.; Ciancaleoni, G.; Zuccaccia, C.; Zuccaccia, D.

Macchioni, A. *Chem. Commun. (Cambridge, UK)* **2010**, *46*, 9218. (e) Lalrempuia, R.; McDaniel, N. D.; Müller-Bunz, H.; Bernhard, S.; Albrecht, M. *Angew. Chem., Int. Ed.* **2010**, *49*, 9765. (f) Hettterscheid, D. G. H.; Reek, J. N. H. *Chem. Commun. (Cambridge, UK)* **2011**, *47*, 2712. (g) Brewster, T. P.; Blakemore, J. D.; Schley, N. D.; Incarvito, C. D.; Hazari, N.; Brudvig, G. W.; Crabtree, R. H. *Organometallics* **2011**, *30*, 965. (h) Schley, N. D.; Blakemore, J. D.; Subbaiyan, N. K.; Incarvito, C. D.; D'Souza, F.; Crabtree, R. H.; Brudvig, G. W. *J. Am. Chem. Soc.* **2011**, *133*, 10473. (i) Dzik, W. I.; Calvo, S. E.; Reek, J. N. H.; Lutz, M.; Ciriano, M. A.; Tejel, C.; Hettterscheid, D. G. H.; de Bruin, B. *Organometallics* **2011**, *30*, 372.

(5) (a) Ellis, W. C.; McDaniel, N. D.; Bernhard, S.; Collins, T. J. *J. Am. Chem. Soc.* **2010**, *132*, 10990. (b) Yin, Q.; Tan, J. M.; Besson, C.; Geletii, Y. V.; Musaev, D. G.; Kuznetsov, A. E.; Luo, Z.; Hardcastle, K. I.; Hill, C. L. *Science* **2010**, *328*, 342. (c) Stracke, J. J.; Finke, R. G. *J. Am. Chem. Soc.* **2011**, *133*, 14872.

(6) For example: (a) Grotjahn, D. B.; Groy, T. L. *J. Am. Chem. Soc.* **1994**, *116*, 6969. (b) Miranda-Soto, V.; Grotjahn, D. B.; DiPasquale, A. G.; Rheingold, A. L. *J. Am. Chem. Soc.* **2008**, *130*, 13200. (c) Miranda-Soto, V.; Parra-Hake, M.; Morales-Morales, D.; Toscano, R. A.; Boldt, G.; Koch, A.; Grotjahn, D. B. *Organometallics* **2005**, *24*, 5569.

(7) McDaniel, N. D.; Bernhard, S. *Dalton Trans.* **2010**, 39, 10021.

(8) (a) Nahor, G. S.; Hapiot, P.; Neta, P.; Harriman, A. *J. Phys. Chem.* **1991**, *95*, 616. (b) Nakagawa, T.; Beasley, C. A.; Murray, R. W. *J. Phys. Chem. C* **2009**, *113*, 12958. (c) Hoertz, P. G.; Kim, Y.-I.; Youngblood, W. J.; Mallouk, T. E. *J. Phys. Chem. B* **2007**, *111*, 6845. (d) Nakagawa, T.; Bjorge, N. S.; Murray, R. W. *J. Am. Chem. Soc.* **2009**, *131*, 15578. (e) Yagi, M.; Tomita, E.; Sakita, S.; Kuwabara, T.; Nagai, K. *J. Phys. Chem. B* **2005**, *109*, 21489. (f) Zhao, Y.; Hernandez-Pagan, E. A.; Vargas-Barbosa, N. M.; Dysart, J. L.; Mallouk, T. E. *J. Phys. Chem. Lett.* **2011**, *2*, 402. (g) Sivasankar, N.; Weare, W. W.; Frei, H. *J. Am. Chem. Soc.* **2011**, *133*, 12976. (h) Blakemore, J. D.; Schley, N. D.; Olack, G. W.; Incarvito, C. D.; Brudvig, G. W.; Crabtree, R. H. *Chem. Sci.* **2011**, *2*, 94.

(9) (a) Nair, V.; Deepthi, A. *Chem. Rev.* **2007**, *107*, 1862. (b) Binnemans, K. In *Handbook on the Physics and Chemistry of Rare Earths*; Gschneider, K. A., Bünzli, J.-C. G., Pecharsky, V. K., Eds.; Elsevier: Amsterdam, 2006; Vol. 36, p 281.

(10) (a) Yoshida, M.; Masaoka, S.; Abe, J.; Sakai, K. *Chem. Asian J.* **2010**, *5*, 2369. (b) Wasylenko, D. J.; Ganesamoorthy, C.; Henderson, M. A.; Berlinguette, C. P. *Inorg. Chem.* **2011**, *50*, 3662.

(11) A reviewer expressed concern that WOC performance can be sensitive to the presence of organic cosolvents. We note that, with the exception of **2a**, all of the catalysts studied here dissolved sufficiently well in water alone that no cosolvent was needed.

(12) See SI for full details. (a) See SI p S4 for discussion of why **3b** and **4b** were made. (b) NMR and MS results (SI pp S71–S274) are discussed in detail on SI pp S58–S70. (c) These percentages include both **4b** and an aquo complex from exchange of CH_3CN .¹² (d) $\text{H}^{13}\text{CO}_2\text{H} + \text{CAN}$ gives $^{13}\text{CO}_2$ (Figure S40).^{12b}

(13) (a) Heidt, L. J.; Berestecki, J. *J. Am. Chem. Soc.* **1955**, *77*, 2049. (b) Hardwick, T. J.; Robertson, E. *Can. J. Chem.* **1951**, *29*, 818. (c) Yu, P.; O'Keefe, T. J. *J. Electrochem. Soc.* **2006**, *153*, C80. (d) Guillou, N.; Auffrédic, J. P.; Louër, D. *J. Solid State Chem.* **1994**, *112*, 45.

(14) (a) Reviewers are thanked for pointing out that the UV–vis bands could be due to molecular species with differing oxidation states or ligands, but we argue that NPs explain the data seen in Figures 1, 2, S25, and S26. (b) Determining absorbance value rigorously is difficult because baselines are hard to define, but we appreciate a suggestion to make the useful comparison.

(15) A control experiment in which **6** was added to CAN (5 equiv) and HNO_3 (20 equiv) gave similar results (Table S1), suggesting that the acidity of CAN alone does not account for catalyst activation.

(16) Examples: Park-Gehrke, L. S.; Freudenthal, J.; Kaminsky, W.; DiPasquale, A. G.; Mayer, J. M. *Dalton Trans.* **2009**, 1972. Heiden, Z. M.; Rauchfuss, T. B. *J. Am. Chem. Soc.* **2007**, *129*, 14303. Competitive intermolecular oxidation of alkane C–H bonds: Zhou, M.; Schley, N. D.; Crabtree, R. H. *J. Am. Chem. Soc.* **2010**, *132*, 12550.